Journal of proteome research

Article

pubs.acs.org/jpr

Exploring Site-Specific N-Glycosylation of HEK293 and Plant-Produced Human IgA Isotypes

Kathrin Göritzer,[†] Daniel Maresch,[‡] Friedrich Altmann,[‡] Christian Obinger,[‡] and Richard Strasser*[,†]

[†]Department of Applied Genetics and Cell Biology, University of Natural Resources and Life Sciences, Muthgasse 18, A-1190 Vienna, Austria

[‡]Department of Chemistry, Division of Biochemistry, University of Natural Resources and Life Sciences, Muthgasse 18, A-1190 Vienna, Austria

Supporting Information

ABSTRACT: The full potential of recombinant Immunoglobulin A as therapeutic antibody is not fully explored, owing to the fact that structure−function relationships of these extensively glycosylated proteins are not well understood. Here monomeric IgA1, IgA2m(1), and IgA2m(2) variants of the anti-HER2 antibody (IgG1) trastuzumab were expressed in glyco-engineered *Nicotiana benthamiana* plants and in human HEK293-6E cells. All three IgA isotypes were purified and subjected to biophysical and biochemical characterization. While no differences in assembly, antigen binding, and glycosylation occupancy were observed, both systems vary tremendously in terms of glycan structures and heterogeneity of glycosylation. Mass-spectrometric analysis of site-specific glycosylation revealed that plant-produced IgAs carry mainly complex-type biantennary N-glycans. HEK293-6E-produced IgAs, on the contrary, showed very heterogeneous N-glycans with high levels of sialylation, core-fucose, and the presence of branched structures. The site-specific analysis revealed major differences between the individual N-glycosylation sites of each IgA subtype. Moreover, the proline-rich hinge region from HEK293-6E cell-derived IgA1 was occupied with mucin-type O-glycans, whereas IgA1 from *N. benthamiana* displayed numerous plant-specific modifications. Interestingly, a shift in unfolding of the CH2 domain of plant-produced IgA toward lower temperatures can be observed with differential scanning calorimetry, suggesting that distinct glycoforms affect the thermal stability of IgAs.

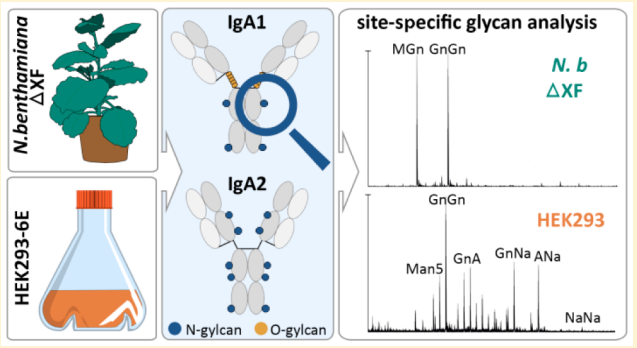

KEYWORDS: *glycosylation, IgA, HEK293-6E, HER2, Nicotiana benthamiana, monoclonal antibody, recombinant glycoprotein*

INTRODUCTION

Therapeutic monoclonal antibodies are the fastest growing class of recombinant biopharmaceuticals. Apart from the most commonly used immunoglobulin G (IgG), other antibody isotypes like IgAs have gained attention as potential candidates for treatment of cancer.[1−3] Human IgA occurs in two subclasses, IgA1 and IgA2, and for IgA2 there are two major allotypes (IgA2m(1) and IgA2m(2)). The different human IgA subtypes differ mainly in the length of their hinge region, disulfide bridges, type, and number of attached glycans.

Notably, all immunoglobulins are glycosylated to varying degrees and glycosylation is an important posttranslational modification that affects many properties of proteins including folding, stability, subcellular fate, and interaction with other proteins. The IgG1 heavy chain has a single asparagine (N)-linked glycan at Asn297 in the CH2 domain. Different types of IgG glycans are well known to modulate antibody function by affecting the binding affinity to receptors on immune cells. Nonfucosylated IgGs display increased affinity for the human FcγIIIA receptor and thus have enhanced effector functions like antibody-dependent cell-mediated cytotoxicity.[4,5] Heavily sialylated IgG antibodies, on the contrary, display an anti-inflammatory and immunomodulatory activity.[6] Therefore, the composition of the Fc glycans is highly important for a specific immunotherapy and a critical parameter of product quality for the biopharmaceutical industry.[7]

Surprisingly, despite the great importance of IgG glycosylation, little is known about the role of glycans for other Ig isotypes. In contrast with IgGs, the other Ig classes including both IgA subclasses are more heavily glycosylated with IgA1, IgA2m(1), and IgA2m(2) carrying two, four, and five N-glycans. Additionally, human IgA1 exhibits up to six O-glycans within its extended hinge region (Figure 1). While IgD, IgE, and IgM have a conserved N-glycosylation site that shares a similar glycan−polypeptide interaction as described for Asn297 from IgG1, an analogous N-glycan appears absent from the IgA alpha chain.[8] Instead of stabilizing intramolecular interactions between the two alpha chains, the N-glycan in the IgA1 CH2 domain is located at the surface of the protein and may have a

Received: March 3, 2017
Published: May 18, 2017

DOI: 10.1021/acs.jproteome.7b00121
J. Proteome Res. 2017, 16, 2560−2570

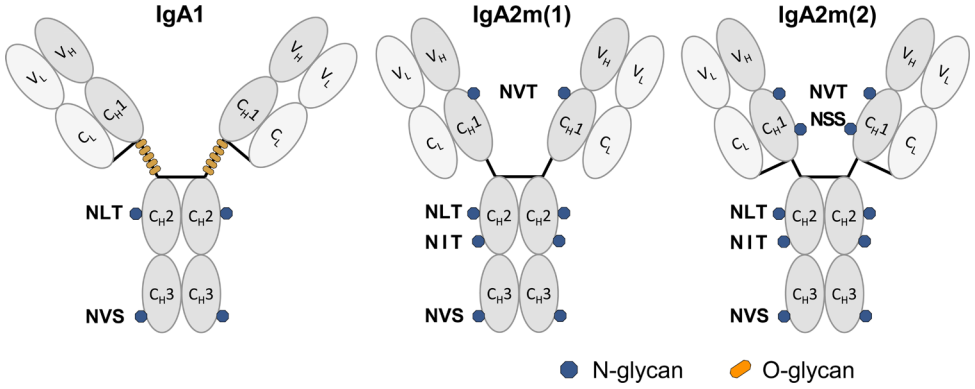

Figure 1. Schematic illustration of structure and glycosylation sites of the IgA isotypes IgA1, IgA2m(1), and IgA2m(2). The light chain is colored in light gray and the heavy chain in dark gray. N-glycans found in the different isotypes are indicated by blue dots. The O-glycans specific for the elongated hinge-region of IgA1 are indicated by orange dots.

completely different biological function. Interestingly, recombinant IgAs are rather short-lived in serum, which is a major drawback for therapy.[9] Similar to other glycoproteins, the rapid clearance depends on the exposure of distinct terminal glycan residues and their recognition by lectin-type receptors. The Ashwell-Morell and other endocytic lectin receptors may be responsible for the fast clearance of IgAs as part of a constitutive mechanism for protein turnover.[10−12] A specific role of glycans for IgA in vivo stability is consistent with a recent report that found an extended serum half-life of recombinant IgAs when the sialic acid content was increased.[13] While the O-glycans in the IgA1 hinge region may also contribute to in vivo stability,[9] it has been proposed that the O-glycans provide additional rigidity[14,15] and are involved in the interaction with endogenous receptors or pathogens.[16,17]

Aside from these findings, little is known about the biological role of individual glycans on the different IgA subtypes. Several recent studies have addressed the IgA glycosylation and its relation to function in the context of therapeutic applications.[13,18−20] These recombinant monomeric IgAs were derived from different expression hosts including plant-based and mammalian-cell culture expression systems. However, the capacity of different expression hosts was not systematically analyzed for the different IgA subtypes, and an in depth site-specific N-glycosylation analysis of all recombinant IgA subtypes is missing. Importantly, MS-based glycopeptide analysis of different heavily glycosylated Ig subtypes revealed pronounced site-specific glycan heterogeneity.[21−24]

For glycan structure−function studies as well as for glycoengineering attempts to improve the efficacy of glycoprotein therapeutics, the information about site-specific N-glycosylation is absolutely essential. This approach is more challenging but reveals important information that is completely lost when glycans are released from the protein for subsequent analysis. Here we produced recombinant anti-HER2 IgA1, IgA2m(1), and IgA2m(2) allotypes in two well-established expression hosts. We expressed all three IgA variants in the widely used human embryonic kidney (HEK293) cells and the glycoengineered *Nicotiana benthamiana* plant-based system, that is, for example, used to manufacture the ZMapp antibody cocktail against Ebola virus infections.[25] The recombinant IgA subtypes were purified, biochemically and biophysically characterized, and subjected to comprehensive site-specific glycosylation analysis to reveal common features as well as differences that may have implications for their function.

MATERIALS AND METHODS

Construct Design and Cloning

The codon-optimized genes of the heavy chains and light chain required for expression of the three different IgA isotypes in *N. benthamiana* and HEK293-6E cells were synthesized by GeneArt (Thermo Fisher Scientific, USA). Therefore, the variable regions of IgA1 (AAT74070.1), IgA2m(1) (AAT74071.1), and IgA2m(2) (AAB30803.1) heavy chains (α-HC) and the kappa light chain (κ-LC) (AAA5900.1) were replaced with the variable regions of the HER2-binding IgG-antibody Trastuzumab (1N8Z_A, 1N8Z_B).[26] Sequences for expression in *N. benthamiana* were flanked with the signal peptide from barley alpha-amylase (AAA98615) and the restriction sites XhoI and AgeI. The synthesized DNA was then amplified by PCR with the primers "Strings_7F (CTTCCGGCTCGTTTGACCGGTATG)/Strings_8R (AAAAACCCTGGCGCTCGAG)", and the constructs were separately cloned into the AgeI/XhoI sites of the binary vector pEAQ-HT.[27] Sequences of the heavy chains and the kappa light chain used for the expression in HEK293-6E were flanked with the signal peptides "MELGLSWIFLLAILKGVQC" and "MDMRVPAQLLGLLLLWLSGARC", respectively, and the restriction sites *Xba*I and *Bam*HI. The synthesized DNA was amplified by PCR with the primers "Strings_9F (CTTCCGGCTCGTTTGTCTAGA)/Strings_2R (AAAAACCCTGGCGGGATCC)". The corresponding genes for the heavy chains and the kappa light chain were then separately cloned into the *Xba*I/*Bam*HI sites of the mammalian vector pTT5 (National Research Council of Canada).[28]

Recombinant Production of IgA Isotypes in *N. benthamiana*

The pEAQ-HT plant expression vectors containing the alpha chains and the kappa light chain were transformed into *Agrobacterium tumefaciens* strain UIA143. Agrobacteria were grown overnight and diluted in infiltration buffer (10 mM MES, 10 mM $MgSO_4$, and 0.1 mM acetosyringone) to an OD_{600} of 0.15. Syringe-mediated agroinfiltration was used for transient cotransfection of the kappa light chain and the corresponding alpha heavy chain of 5 to 6 weeks old *N. benthamiana* ΔXT/FT plants.[29] For purification of the different IgA isotypes, 50 g of leaf material was harvested 4 days post-infiltration, snap-frozen in liquid nitrogen, and grinded. Homogenized leaf material was transferred to 200 mL of ice-cold extraction buffer (0.1 M TRIS, 0.5 M NaCl, 1 mM EDTA, 40 mM ascorbic acid, 2% (w/

DOI: 10.1021/acs.jproteome.7b00121
J. Proteome Res. 2017, 16, 2560−2570

v) immobilized polyvinylpoly pyrrolidone (PVPP), pH 6.8). The crude leaf extract was centrifuged at 25 000*g* for 20 min at 4 °C, passed through a Miracloth filter (Merck Millipore, Germany), and centrifuged again. The clarified extract was additionally filtrated through filters with pore sizes of 12−8 μm, 3 to 2 μm (Rotilabo round-filters, Roth, Germany), and 0.45 μm (Durapore membrane filter, Merck Millipore, Germany).

Recombinant Production of IgA Isotypes in HEK293-6E Cells

The HEK293-6E cell line that constitutively expresses the Epstein−Barr virus nuclear antigen 1 of the Epstein−Barr virus was licensed from the National Research Council (NRC) of Canada.[28] The suspension cells were cultivated and transfected according to the manufacturer's manual in F17 medium supplemented with 0.1% Pluronic F-68, 4 mM L-glutamine (Life Technologies, Germany), and 50 mg/L G418 (Biochrom, Germany). The cells were maintained in shaker flasks at 37 °C in a humidified atmosphere with 5% CO_2 on an orbital shaker never exceeding a cell density of 2×10^6 cells/mL. For transient transfection of a 200 mL culture, cells were brought to a concentration of 1.7×10^6 cells/mL. High-quality plasmid preparations of the pTT5 vector coding for the kappa light chain and the different alpha heavy chain were obtained using the PureYield Plasmid Midiprep System (Promega, USA). A total of 200 μg plasmid-DNA, consisting of 100 μg light chain and 100 μg of the respective heavy chain, were mixed with 10 mL of fresh medium. Another 10 mL of fresh medium, containing 2.5 μg/mL linear polyethylenimine (PEI) (Polysciences, Germany), was added to the DNA solution and incubated for 10 min. After adding the DNA/PEI mixture, the cells were incubated for 48 h, supplemented with 0.5% (w/v) tryptone N1 (Organotechnie, France) and further cultivated for 72 h. Supernatant containing the secreted soluble protein was harvested by centrifugation at 25 000*g* for 30 min at 4 °C and additionally filtrated (0.45 μm Durapore membrane filter, Merck Millipore, Germany).

Purification of Recombinant IgAs

Clarified leaf extract from *N. benthamiana* and supernatant of HEK293-6E suspension cells were subjected to a HiScale 16/20 column (GE Healthcare, USA) packed with 3 mL of CaptureSelect IgA affinity resin (Thermo Fisher Scientific, USA) equilibrated with phosphate-buffered saline (PBS) pH 7.4. Proteins were eluted with 0.1 M glycine pH 2.8, followed by immediate addition of 6 μL of 2 M Tris pH 12 to each 1 mL fraction to neutralize the acidic pH from glycine elution. Highly concentrated fractions were pooled and dialyzed against PBS at 4 °C overnight using SnakeSkin Dialysis Tubing with a MWCO of 10 000 kDa (Thermo Fisher Scientific, USA). Finally, the column was regenerated with 0.1 M glycine pH 2.5 and washed with PBS. Pooled protein fractions were then further concentrated using Amicon centrifugal filters with a MWCO of 10 000 kDa (Merck Millipore, Germany) and subjected to size-exclusion chromatography (SEC) on a HiLoad 16/600 Superdex 200 pg column (GE Healthcare, USA) equilibrated with PBS supplemented with 200 mM NaCl.

SDS-PAGE

For reducing or nonreducing SDS-PAGE a total of 5 μg of purified protein was loaded on a 4−15% Mini-PROTEAN TGX gel (Bio-Rad Laboratories, USA) and visualized with Coomassie Brilliant Blue staining.

Binding to Antigen HER2

The purified extracellular domain of human HER2 (residues 1−631), which was used for antigen-binding experiments, was generously provided by Elisabeth Lobner (BOKU Vienna). Each well of a medium binding MICROLON 200 96-well plate (Greiner Bio-One Intern., Germany) was coated with 0.5 μg HER2 overnight at 4 °C in coating buffer (0.5 M sodium carbonate/bicarbonate, pH 9.8). Plates were then blocked with PBS plus 2% (w/v) BSA and 0.05% (v/v) Tween 20. Purified IgA1, IgA2m(1), and IgA2m(2) antibodies were diluted to 500 ng/mL in blocking solution, added to the wells in normalized concentrations, and incubated for 1.5 h at room temperature. HRP-labeled antihuman IgA (A0295, Sigma-Aldrich, USA) was added to the wells and incubated 1 h at room temperature. The plates were developed using 5 mg *O*-phenylenediamine dihydrochloride in 10 mL of stable peroxidase substrate buffer (all Sigma-Aldrich, USA). After 20 min of incubation the plates were read on a Wallac 1420 VICTOR2 microplate reader (PerkinElmer, U.K.) at 492 nm.

Size Exclusion Chromatography−Multiangle Light Scattering (SEC−MALS)

To verify the molar mass of purified IgAs, high-performance liquid chromatography (HPLC) coupled to a size-exclusion chromatography column was combined with multiangle light scattering. HPLC (Shimadzu prominence LC20) was equipped with MALS (WYATT Heleos Dawn8+ QELS; software ASTRA6), refractive index detector (RID-10A, Shimadzu), and a diode array detector (SPD-M20A, Shimadzu). Samples were centrifuged (15 000*g*, 10 min, 4 °C) and filtrated through a 0.1 μm Ultrafree-MC filter (Merck Millipore, Germany), and a total of 25 μg protein was injected on a Superdex 200 10/300 GL column (GE Healthcare, USA) equilibrated with Dulbecco's PBS plus 200 mM NaCl, pH 7.4. All experiments were performed at a flow rate of 0.75 mL/min at 25 °C. The performance of molar mass calculation by MALS was verified by the determination of a sample of bovine serum albumin.

Differential Scanning Calorimetry

The thermal stability of the IgA variants was analyzed by differential scanning calorimetry (DSC) using a MicroCal VP-Capillary DSC (Malvern, U.K.). Purified samples were diluted to a concentration of 5 μM and were measured in the temperature range from 20 to 110 °C with a heating rate of 1 °C/min. Buffer baselines were subtracted, normalized for protein concentration, and fitted with a non-2-state thermal unfolding model using the Origin 7 software.

N- and O-Glycan Analysis

Between 5 and 10 μg of purified proteins was loaded on a SDS-PAGE under reducing conditions, and Coomassie Brilliant Blue stained bands were excised, S-alkylated, and digested with trypsin (Promega USA). Glycopeptides were then analyzed by capillary reversed-phase chromatography and electrospray mass spectrometry using a Bruker Maxis 4G Q-TOF instrument. The peptide mixture was dissolved in 15 μL of water, and a volume of 5 μL was analyzed using a Dionex Ultimate 3000 system directly linked to a QTOF instrument (maXis 4G ETD, Bruker) equipped with the standard ESI source in the positive ion, DDA mode (= switching to MSMS mode for eluting peaks). MS scans were recorded (range: 150−2200 *m*/*z*, spectra rate: 0.5 Hz) and the six highest peaks were selected for fragmentation (CID mode). Instrument calibration was performed using ESI calibration mixture (Agilent). For

DOI: 10.1021/acs.jproteome.7b00121
J. Proteome Res. 2017, 16, 2560−2570

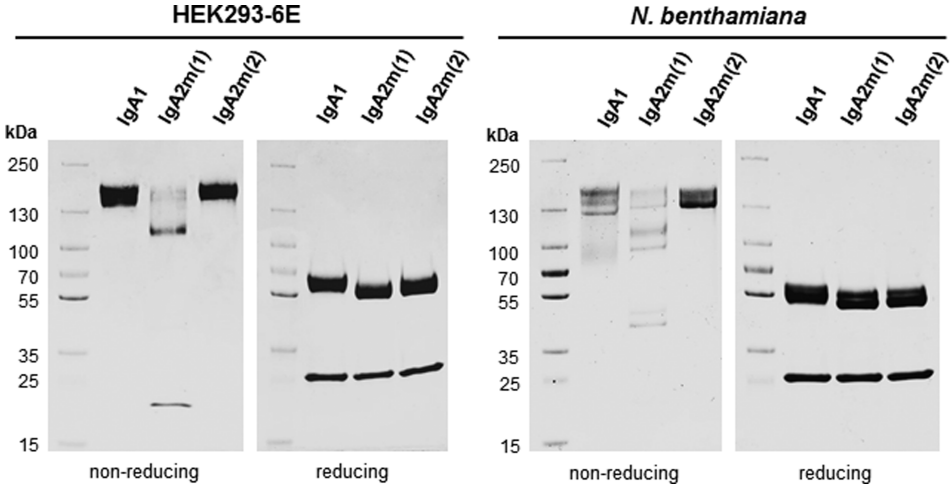

Figure 2. Purity and assembly of recombinantly produced IgA1, IgA2m(1), and IgA2m(2). Purified IgAs produced in *N. benthamiana* and HEK293-6E cells were run on an SDS-PAGE under reducing and nonreducing conditions. Proteins were then detected by Coomassie Brilliant Blue staining.

separation of the peptides a Thermo BioBasic C18 separation column (5 μm particle size, 150 × 0.320 mm) was used. A gradient from 97% solvent A and 3% solvent B (Solvent A: 65 mM ammonium formiate buffer, pH 3.0 (formic acid supplied by Carl Roth; ammonia supplied by VWR BDH Prolabo), B: 100% ACCN (VWR BDH Prolabo)) to 32% B in 45 min was applied, followed by a 15 min gradient from 32% B to 75% B at a flow rate of 6 μL/min at 32 °C.

The analysis files were converted using Data Analysis 4.0 (Bruker) to MGF files, which are suitable to perform MS/MS ion searches with MASCOT (embedded in ProteinScape 3.0, Bruker) for protein identification using the manually annotated and reviewed UniProtKB database. Manual glycopeptide searches were done using DataAnalysis 4.0 (Bruker). MS/MS spectra were used for the verification of the glycopeptides by detection of oxonium ions HexNAc (m/z = 204.1), Hex +HexNAc (m/z = 366.1), and the unique Y1 ion (peptide +HexNAc). For the relative quantification of the different glycoforms, peak areas of EICs (extracted ion chromatograms) of the first four isotopic peaks were summed. All observed charge states and adducts (ammonium) as well as the formation of formylated glycopeptides were considered. Site-specific glycosylation occupancy was calculated using the ratio of deamidated to unmodified peptide determined upon N-glycan release with PNGaseA (Europa Bioproducts).

For the digestion the remaining sample material (10 μL) was dried and resolved in 20 μL of 50 mM ammonium citrate (pH 5.0), and 0.15 mU of enzyme was added and incubated overnight at 37 °C.

RESULTS

Recombinant Production of IgA in Different Expression Hosts

To compare the capacities of plant-based and mammalian-based expression systems, the three IgA isotypes IgA1, IgA2m(1), and IgA2m(2) (Figure 1) were produced in HEK293-6E cells and in the glyco-engineered *N. benthamiana* ΔXT/FT line that almost completely lacks plant-specific β1,2-xylose and core α1,3-fucose residues. For expression of the different IgAs in plants, the leaves of *N. benthamiana* were coinfiltrated with agrobacteria containing the κ-LC and the respective α-HC. Immunoblot analysis and ELISA showed that the highest level of recombinant protein accumulated 4 days postinfiltration (data not shown). For purification of IgA from the crude plant extract, 50 g of leaf material was harvested, extracted, and subjected to affinity chromatography, followed by a SEC step. The preparative SEC profiles thereby revealed the presence of high-molecular-weight aggregates, dimeric IgA, and free heavy chain (data not shown). For further analyses, only fractions containing the monomeric structural unit of IgA were pooled. The final yield of purified monomeric IgA from *N. benthamiana* ranged from 3.5 mg/50 g of fresh weight from leaf for IgA1 and IgA2m(1) to 5 mg/50 g for IgA2m(2). For the expression of IgAs in a mammalian host, 200 mL of a HEK293-6E cell suspension culture was cotransfected with two vectors, encoding the κ-LC and the respective α-HC. The supernatant was collected and subjected to affinity chromatography, followed by SEC. As already seen in the SEC profiles of plant-produced proteins, also IgAs expressed in the HEK293 cell line showed the presence of high-molecular weight-aggregates. Again only fractions containing the monomeric IgA forms were collected. The final yield of IgA from HEK293-6E was in the range of 15 mg/L for all three isotypes.

Characterization of Purified Monomeric IgA Variants

The purified monomeric IgA variants were investigated for their overall assembly and homogeneity using SDS-PAGE and SEC coupled to MALS. Reducing SDS-PAGE of purified IgAs produced in *N. benthamiana* ΔXT/FT and in HEK293-6E cells confirmed the presence of the α-HC and the κ-LC without any degradation products (Figure 2). However, the heavy chain at 55 kDa can be observed as a double band. The distinct bands were cut from the gel and separately analyzed by mass spectrometry (Supplementary Figure S2). Thereby it was shown that the band with a higher molar mass contains more oligomannosidic glycans and has a higher glycosylation occupancy of the C-terminal N-site compared to the band with lower molar mass.

Under nonreducing conditions, IgA1 and IgA2m(2) show a predominant band at a molar mass around 160 kDa representing the fully assembled molecule. The plant -produced IgA2m(1) variant displayed additional bands at 115, 100, and 45 kDa, which likely represent heavy and light chain dimers. The HEK293-derived IgA2m(1) also shows additional bands at 115 and 20 kDa. However, SEC profiles of all IgA variants,

DOI: 10.1021/acs.jproteome.7b00121
J. Proteome Res. 2017, 16, 2560−2570

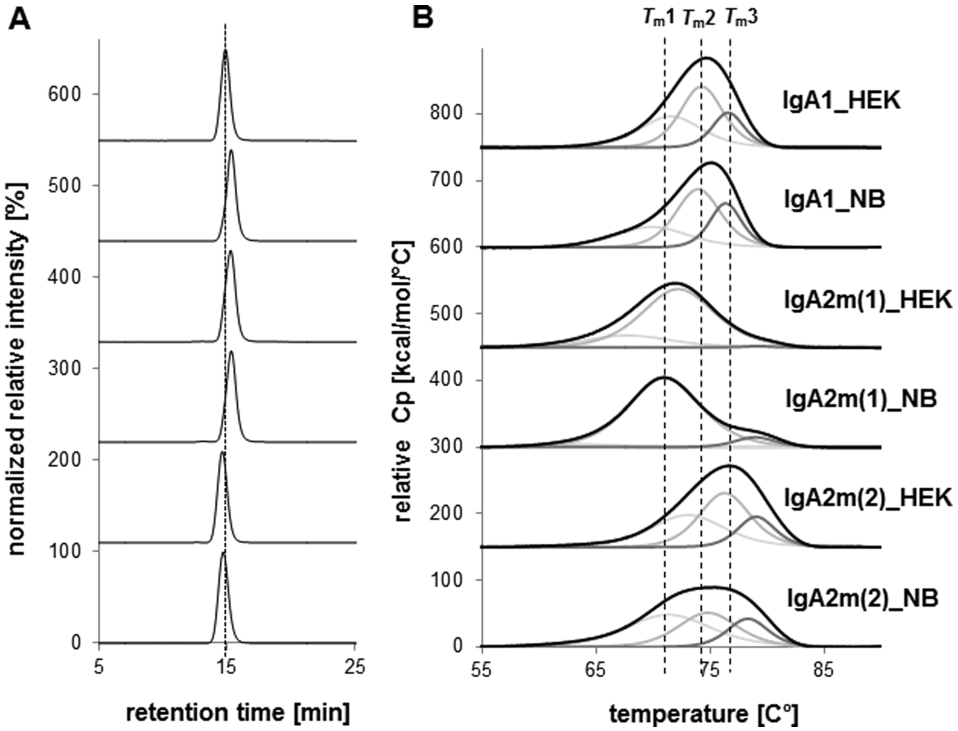

Figure 3. Homogeneity and thermal stability of the IgA isotypes IgA1, IgA2m(1), and IgA2m(2). (A) SE-HPLC measurements of the different IgA isotypes purified from HEK293-6E cells (HEK) and *N. benthamiana* (NB). To facilitate comparison between the different variants the elution time of IgA1 produced in HEK293 cells is marked with dashed lines. (B) Differential scanning calorimetry analysis of IgAs produced in *N. benthamiana* (NB) and HEK293-6E cells (HEK). The black bold lines show representative DSC thermograms, whereas the gray lines are the deconvoluted peaks of each domain transition. For comparison, the three midterm transitions of the CH2, Fab, and CH3 domain (T_m1 = 71.6 ± 0.1 °C, T_m2= 74.3 ± 0.05 °C, and T_m3 = 76.6 ± 0.1 °C) of IgA1 produced in HEK293 cells are marked with dashed lines.

including IgA2m(1) produced in both systems, gave narrow and single monodisperse peaks (Figure 3A). The masses of these peaks of ∼160 kDa were confirmed by MALS and correspond to the fully assembled monomeric forms. Furthermore, no aggregates and no aberrantly assembled IgA variants could be detected.

Next, we investigated the thermal stability of the IgA variants by DSC (Figure 3B). Unfolding of the recombinant IgAs is reflected by a broad endotherm. Analysis and fitting suggested the presence of three independent transitions allowing identification of the transition midpoint temperatures of the CH2 (T_m1), Fab (T_m2), and CH3 (T_m3) domains, as already described for IgG.[30] Immunoglobulin A1 produced in HEK293 cells exhibited melting temperatures at 71.6 ± 0.01, 74.3 ± 0.05, and 76.6 ± 0.1 °C, respectively. The plant-produced counterpart exhibited almost identical T_m2 and T_m3 values, whereas unfolding of the CH2 domain started at a slightly lower temperature.

Comparison of the two IgA2 allotypes shows significant differences in thermal stability with IgA2m(1) being less stable than IgA2m(2). Immunoglobulin A2m(1) produced in HEK293 cells exhibited melting temperatures at 67.9 ± 0.05, 72.3 ± 0.1, and 79.2 ± 0.1 °C, respectively. Similar to IgA1, the plant-produced variant showed almost identical T_m2 and T_m3 values, whereas T_m1 was decreased by ∼4 °C. In the allotype IgA2m(2) produced in HEK293 cells both the CH2 and Fab domains are more stable (T_m1 = 73.1 ± 0.05 and T_m2 = 76.3 ± 0.1 °C), whereas the calculated T_m3 value was almost similar to that of IgA2m(1). The endotherm of the plant-derived variant was broader and the respective T_m values of the three transitions were slightly decreased (Figure 3B). In general, the hierarchy of thermal stability is IgA2m(2) > IgA1 > IgA2m(1). In the plant-derived products the CH2 domain was always slightly destabilized compared with the HEK293-produced variants, whereas the differences in melting temperatures of the Fab and CH3 domains were at most ∼1 °C.

To confirm the functionality of all expressed IgAs, binding to the HER2 antigen was assessed by ELISA and the half maximal effective concentration (EC_{50}) was determined for each recombinant monomeric IgA variant. Thereby it could be shown that the antigen binding behavior of all three IgA isotypes was very similar and independent of the production host (Figure 4).

Glycan Profiles of IgAs Produced in Different Expression Platforms

The observed differences in thermal unfolding of IgA variants from different expression hosts may arise from differences in glycosylation. There are two predicted N-glycosylation sites in the α-HC of IgA1 and four to five N-glycosylation sites in IgA2m(1) and IgA2m(2), respectively. In addition, IgA1 has nine potential O-glycosylation sites in the proline-rich hinge region. To assess the glycosylation status of purified monomeric IgA isotypes produced in *N. benthamiana* or HEK293-6E, the α-HC was subjected to SDS-PAGE and stained with Coomassie Brilliant Blue. The corresponding band was excised, digested with trypsin, and analyzed by LC−ESI−MS for site-specific N-glycosylation and the presence of modifications within the IgA1 hinge region. Furthermore, all samples were additionally digested with PNGase A to release the attached N-glycans. After the PNGase A digestion, the ratios of the resulting deamidated peptides (glycosylated) to

DOI: 10.1021/acs.jproteome.7b00121
J. Proteome Res. 2017, 16, 2560−2570

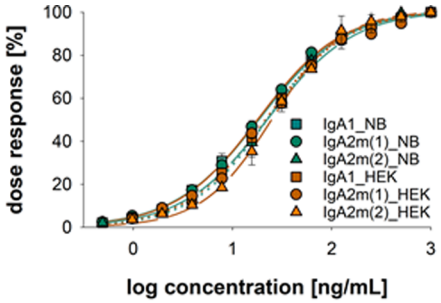

	EC_{50} [ng/mL]		
	IgA1	IgA2m(1)	IgA2m(2)
HEK293-6E	21.8 ± 0.38	22.38 ± 0.25	25.10 ± 0.24
N. benthamiana	18.87 ± 0.23	18.20 ± 0.22	22.40 ± 0.23

Figure 4. Binding of IgA variants to HER2. Determination of EC_{50} values of IgA isotypes produced in *N. benthamiana* and HEK293 cells to the extracellular domain of HER2 by ELISA. Each value is the mean ± standard deviation from three independent measurements.

unmodified (nonglycosylated) peptides were quantified to determine the glycosylation efficiency of both expression systems at each N-glycosylation site. All predicted N-glycosylation sites were found to be occupied in all IgA variants (Figure 5). Both systems were equally efficient in attachment of N-glycans and all except the C-terminal N-glycosylation site were almost fully glycosylated. The C-terminal N-glycosylation site present in the tailpiece of all IgAs was only 40−60% glycosylated. Although the two hosts do not significantly differ in their N-glycosylation efficiency, both systems differ tremendously in terms of structural composition of attached glycans. The N-glycans found on plant-produced IgA showed a comparably homogeneous profile, with biantennary complex-type structures like $GlcNAc_1Man_3GlcNAc_2$ (MGn/GnM) and $GlcNAc_2Man_3GlcNAc_2$ (GnGn) as major glycoforms (Figure 6 and Table 1). The presence of N-glycan structures with a single terminal GlcNAc residue in *N. benthamiana*-derived IgA variants is in accordance with previous data, suggesting an incomplete processing of the NLT site in the CH2 domain by *N*-acetylglucosaminyltransferase II (GnTII).[31] Furthermore, variable amounts of oligomannosidic structures were detected along with small amounts of complex N-glycans carrying the plant-specific core α1,3-fucose. This modification results from the incomplete silencing of core α1,3-fucosyltransferase in the *N. benthamiana* ΔXT/FT line.[29] HEK293-produced IgAs showed clear site-specific differences and more diverse N-glycan profiles compared with plant-produced IgAs. Several of the detected glycopeptide masses correspond to complex N-glycan compositions that could not be distinguished because of the same theoretical mass. These structures include different branched complex N-glycans with or without a bisecting GlcNAc (Table 1). However, the predominant glycoforms found attached to the NVT, NSS, NLT, and NIT sites of the respective IgA isotype are biantennary complex-type structures with high levels of galactosylation and up to 30% sialylation. The NVS glycosylation site in the C-terminal tailpiece comprises more highly branched complex N-glycans with high levels of incompletely galactosylated triantennary glycans carrying a bisecting GlcNAc or tetraantennary glycans. Only a small degree of sialylation was found at this N-glycosylation site. The N-glycans from HEK293-derived IgAs also vary in the attachment of core-fucose, which is present on all complex N-glycans except those found on the NLT site from the CH2 domain.

The most significant difference between the two expression systems *N. benthamiana* ΔXT/FT and HEK293-6E was the modification of the proline-rich hinge region of IgA1. O-glycans found on IgA1 produced in mammalian cells are a combination of mucin-type core structures with a maximal occupation of six out of nine potential O-glycosylation sites (Figure 7). On the hinge region of plant-produced recombinant IgA1 we detected the conversion of proline residues to hydroxyproline and the presence of additional pentoses, presumably representing attached arabinose chains.

Taken together, the site-specific analysis of glycosylation revealed major differences between individual N-glycosylation sites on the heavy chain of each IgA subtype. Although the glycan composition differed considerably between the plant and mammalian expression systems, the site-specific features appear conserved.

DISCUSSION

The role of glycosylation for immunoglobulins like IgA is still not well understood. In recent studies, the potential of recombinant anti-HER2 IgAs has been investigated.[13,19] These studies suggest that defined glycan modifications, such as the attachment of terminal sialic acid residues, are critical to increase the half life of IgAs in vivo. However, because of the absence of site-specific glycan analysis, important information was not revealed. Moreover, in addition to well-established mammalian cell systems, the use of plant-based production for recombinant immunoglobulins is gaining more and more attention as plants allow the production of customized

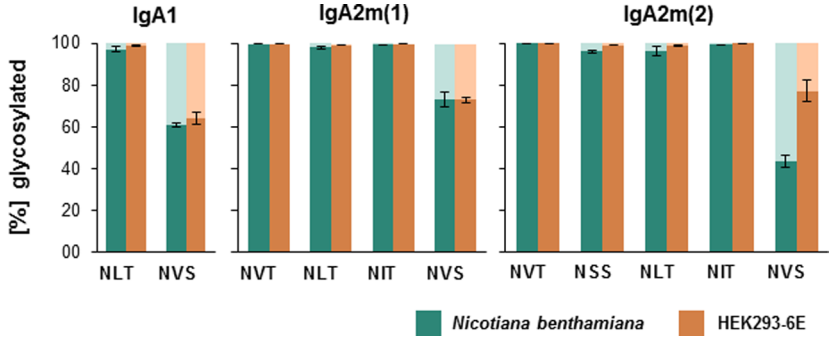

Figure 5. N-glycosylation site occupancy of IgA isotypes produced in HEK293-6E cells and in *N. benthamiana*. Each value is the mean ± standard deviation from two independent experiments.

DOI: 10.1021/acs.jproteome.7b00121
J. Proteome Res. 2017, 16, 2560−2570

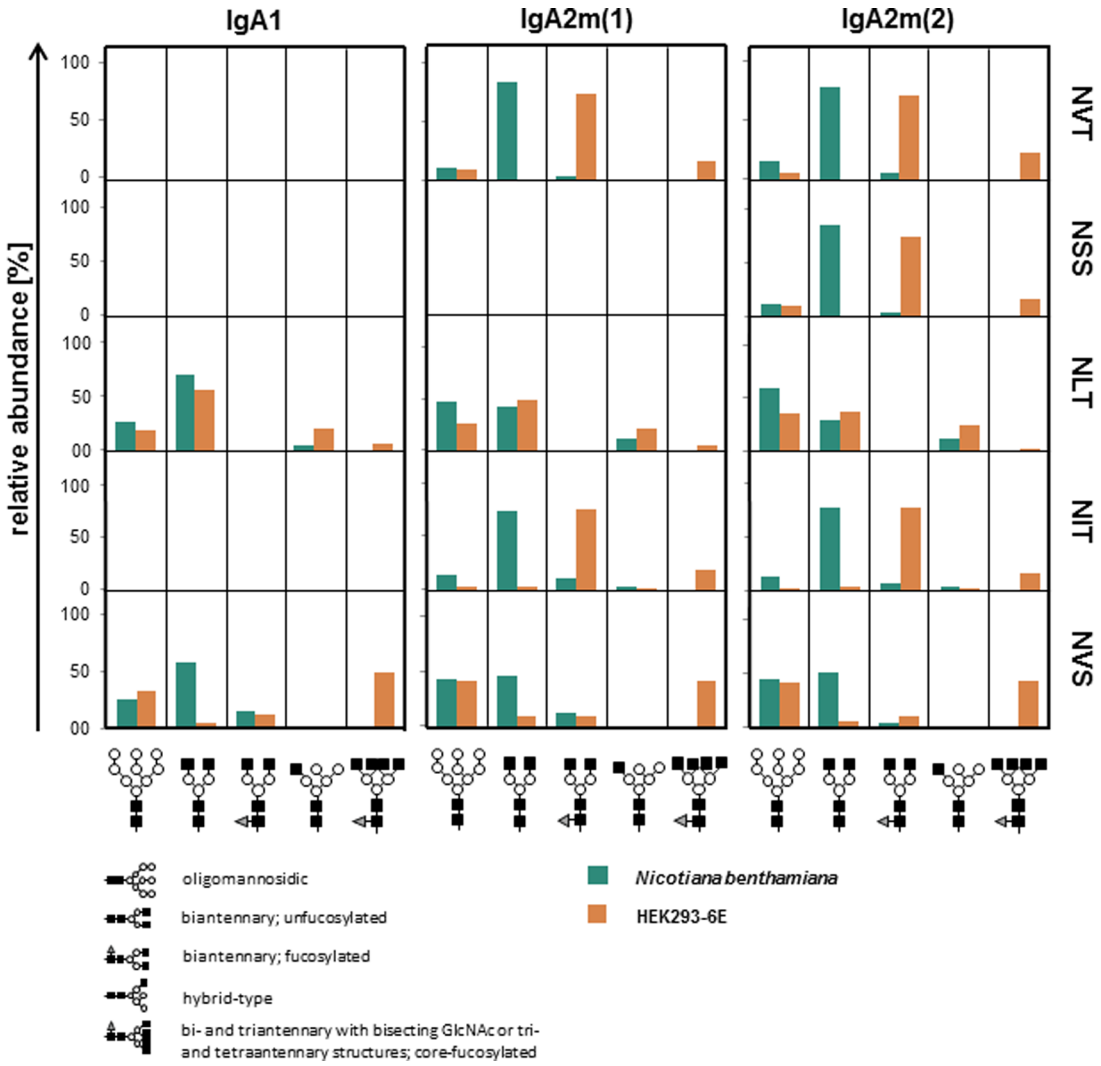

Figure 6. Relative abundance of N-glycans found on IgA isotypes produced in *N. benthamiana* and HEK293-6E cells. Glycoforms are grouped from left to right into oligomannosidic, biantennary without core-fucose, biantennary with core-fucose, hybrid-type, and bi- and triantennary with bisecting GlcNAc or triand tetranatennary structures with core-fucose.

homogeneous glycans with few engineering steps.[18,22,25,31−33] Here we compared the two different systems and performed a comprehensive analysis of the glycans at each site of three anti-HER2 IgA subtypes.

In both systems an almost complete occupancy with N-glycans was observed on all sites except the one in the C-terminal tailpiece, demonstrating that glycosylation efficiency was essentially the same. This finding is remarkable, as there are differences in the composition and function of the plant and mammalian oligosaccharyltransferase complexes that catalyze the transfer of the oligosaccharide to asparagine residues.[34] The incomplete glycosylation of the C-terminal tailpiece is likely caused by inefficient posttranslational glycosylation mediated by a specific catalytic subunit of the oligosaccharyltransferase complex.[35] All other sites are presumably cotranslationally glycosylated while the polypeptide is still synthesized.

As a consequence of the limited N-glycan processing repertoire in the Golgi, the glycan diversity found on plant-produced recombinant IgAs was clearly reduced. In particular, plant N-glycans lack tri- and tetraantennary structures, bisecting GlcNAc, β1,4-galactose, and capping with sialic acid. Those glycan modifications were all detected on the HEK293-derived IgA, resulting in increased heterogeneity. In addition, the HEK293-derived IgA may also contain smaller amounts of *N*-acetyllactosamine-repeat containing N-glycans that were not distinguished from some tri- and tetraantennary N-glycans and contribute to heterogeneity.

Despite having completely identical amino acid sequences, plant- and human-cell-derived IgA subtypes exhibited differences in thermal stability. Because the respective variants differ only in glycosylation, we propose that observed differences in T_m values are related to the presence of distinct glycoforms causing the variation in thermal stability. Comparable DSC measurements are not available for recombinant or native IgA molecules, but data from thermal unfolding of IgG showed that oligomannosidic and deglycosylated forms were less stable.[36] However, because of the different positioning (exposed for IgA, confined between the two CH2 domains for IgG) of the Fc oligosaccharide no direct comparison can be made. Nevertheless, in the plant-derived IgA variants the CH2 domain was always destabilized by about 2−4 °C compared with the HEK293 produced variants, whereas the differences in T_m values of the Fab and CH3 domains were very small. The significant difference in thermal stability of the Fab and CH2

DOI: 10.1021/acs.jproteome.7b00121
J. Proteome Res. 2017, 16, 2560−2570

Table 1. Quantification of the Relative Abundance of N-Glycans Detected on IgA Isotypes Produced in *N. benthamiana* and HEK293-6E Cells[a]

			IgA1				IgA2m(1)								IgA2m(2)									
			N.B		HEK		N.B				HEK				N.B					HEK				
			NLT	NVS	NLT	NVS	NVT	NLT	NIT	NVS	NVT	NLT	NIT	NVS	NVT	NSS	NLT	NIT	NVS	NVT	NSS	NLT	NIT	NVS
		% unglycosylated	2.9	38.9	1.1	35.9	<0.1	2.0	0.7	26.6	<0.1	0.7	<0.1	26.8	<0.1	3.9	3.7	0.6	56.5	<0.1	1.0	0.8	<0.1	22.9
oligomannosidic	Man4		0.4		0.4			0.7	0.5			0.3					0.8	0.8				0.3		
	Man5		1.2	0.3	4.4	14.0	0.5	2.0	0.5	0.8	9.4	6.1	2.0	25.1	1.2	0.4	2.8	0.8	0.3	6.1	2.6	7.3	2.0	26.1
	Man6		6.2	1.7	3.1	8.5	0.7	6.8	0.4	1.5		5.0		9.2	1.2	0.9	7.9	0.5	3.7			6.0		8.1
	Man7		4.8	9.9	5.0	4.8	2.7	11.4	1.4	14.2		7.6		2.8	3.8	2.9	13.8	1.4	13.3			10.5		2.5
	Man8		7.6	10.8	2.8	4.3	5.4	13.2	6.5	18.6		4.1		2.7	4.6	5.9	14.6	5.4	18.2			6.1		2.7
	Man9		5.4	2.7	2.4	1.8	2.5	12.6	4.1	6.7		3.2		1.4	4.9	2.3	18.0	3.9	9.0			5.7		1.8
	Man9+1Hex		0.2	0.5				0.3	0.1	0.6						0.3	0.5	0.2	0.3					
biantennary - unfucosylated	MM		6.3	1.2			10.2	4.2	12.7						18.7	10.7	2.6	14.9						
	MGn		30.8	3.7	2.8		20.0	22.8	20.0	5.4		2.4	1.1		13.3	16.6	17.4	18.4	7.5			2.1	1.3	
	GnGn		31.9	53.5	16.6	1.7	54.2	14.6	40.7	40.5		15.3	2.0	3.3	46.0	47.6	9.7	43.3	43.2			13.2	2.6	2.0
	GnA				8.7							7.6										6.3		
	AA				3.6							2.5										2.1		
	GnNa				11.0							10.8										7.3		
	ANa				11.4	2.6						8.5		5.0								4.9		3.1
	NaNa				1.4							1.6										0.7		
biantennary - fucosylated	MMF								2.1							2.6		1.6						
	MGnF								2.7				3.8			3.0		1.4			2.8		3.8	
	MAF												1.8										1.9	
	GnGnF			15.8		5.7	3.9		6.0	11.7	23.8		25.6	8.0	6.2	6.9		4.1	4.4	25.3	27.7		24.9	7.2
	GnAF										15.4		14.6							13.6	13.6		15.0	
	AAF					2.9					10.9		10.4	0.7						7.0	7.0		9.9	1.3
	GnNaF										6.2		5.2							7.0	5.2		6.8	
	ANaF					3.8					15.5		12.3	0.2						14.9	8.1		13.4	1.6
	NaNaF										2.1		1.4							3.2	1.0		1.6	
hybrid type	Man4Gn / MA		2.9		4.7			5.3	1.2			4.9					5.2	1.4				5.2		
	Man5Gn		2.4		7.7			6.0	0.8			8.1	0.8				6.5	1.3				10.7	1.0	
	Man5Gn+1Hex				2.3				0.3			2.5						0.4				3.1		
	Man4Na				3.8							3.4										3.6		
	Man5Na				1.3							1.8										2.3		
biantennary with bisecting GlcNAc and/or triantennary	GnGnbi / GnGnGn				4.4							3.0										1.8		
	GnAbi / GnGnA				2.1							1.3										0.9		
	GnGnFbi / GnGnGnF					10.9					7.7		9.1	9.2						11.4	14.3		7.2	9.2
	GnAFbi / GnGnAF					4.4					5.8		5.9	3.2						6.4	9.8		5.2	3.8
	AAFbi / GnAAF					2.1					3.3		2.9	4.9						5.0	3.5		2.6	4.0
	AAAF					1.3							1.0	1.3							0.7		0.9	1.4
	AANaF					2.4								1.4										1.3
	GnNaFbi / GnGnNaF																				1.9			
	ANaFbi / GnANaF																				1.1			
triantennary with bisecting GlcNAc and/or tetraantennary	GnGnGnFbi / GnGnGnGnF					11.2								8.8										7.5
	GnGnAFbi / GnGnGnAF					4.0								4.1										5.1
	GnAAFbi / GnGnAAF					2.1								1.9							0.6			3.0
	AAAFbi / GnAAAF					2.4								1.1										1.8
	AAAAF					1.6								1.2										1.0
	AANaFbi / GnAANaF					0.4								2.0										1.5
	AAANaF					4.2								0.6										2.0
	GnGnGnGnFbi					2.9								1.8										1.7

Hexose GlcNAc Mannose Fucose Galactose Sialic acid

[a]N-glycans are abbreviated according to the ProGlycAn system (www.proglycan.com). The symbols for the monosaccharides are drawn according to the nomenclature from the Consortium for Functional Glycomics. Please note that *N*-acetyllactosamine repeats may also be present on HEK293-6E cell-derived IgA N-glycans, which cannot be distinguished from some tri- and tetraantennary N-glycans by the used MS analysis.

DOI: 10.1021/acs.jproteome.7b00121
J. Proteome Res. 2017, 16, 2560−2570

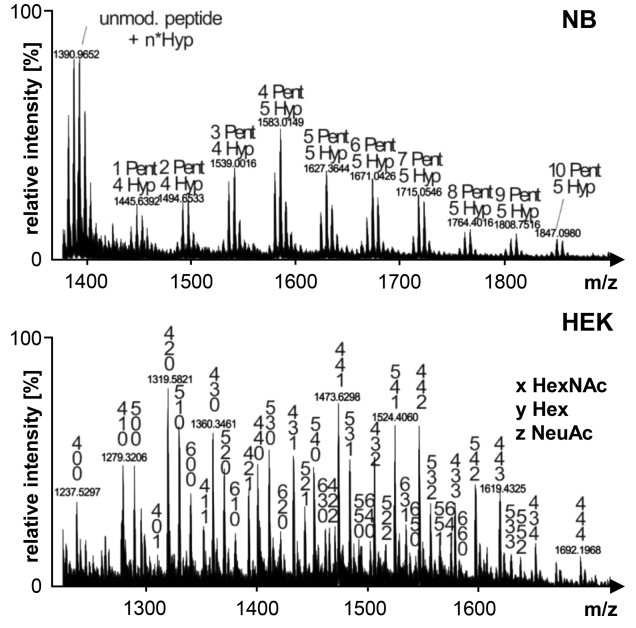

Figure 7. O-glycosylation profiles of *N. benthamiana* (NB) and HEK293-6E (HEK)-derived recombinant IgA1. Mass spectra of the hinge region peptide (HYTNPSQDVTVPCPVPSTPPTPSPSTPPTP-SPSCCHPR) are shown ($[M+3H]^{3+}$ for NB and $[M+4H]^{4+}$ for HEK). Glycosylated peaks are indicated: pentoses (Pent), hydroxyproline (Hyp), putative *N*-acetylgalactosamine (HexNAc), hexoses (Hex), and sialic acid residues (NeuAc).

domains between the two IgA2 isoforms seems to be related to the presence of the IgA2m(2)-typical disulfide bridge between the CL and CH1 domains (Figure 1).

Plants do not have a functional mucin-type O-glycosylation pathway[37,38] but perform plant-specific modifications. Thereby proline is converted to hydroxyproline, followed by the addition of arabinoses to the hydroxyproline-residues. Apart from *N. benthamiana,* these plant-type modifications have been previously described for human IgA1 derived from maize seeds.[39] While it will be of interest to determine the effect of the plant-type O-glycosylation on the biophysical properties and stability of IgA1, the hydroxyproline residues and attached glycan moieties may elicit an unwanted immune response when present on recombinant IgA1[40] and hamper O-glycan engineering approaches. The importance of hinge region modifications is well documented for IgA nephropathy, a kidney disease where autoantibodies against O-glycans from the IgA1 hinge region lead to glomerular immune complex deposits.[41] Strategies to eliminate the unwanted prolyl-4-hydroxylase activity have been successfully applied to a moss-based expression system[42] and need to be adopted for the commonly used *N. benthamiana*-based system.

Recombinant IgA subtypes from the human cell line displayed a considerable number of diverse complex N-glycans and clear site-specific differences like the lack of core α1,6-fucose on the conserved N-glycan located in the CH2 domain. The absence of this modification has also been reported for serum or CHO-produced IgA and presumably results from steric hindrance of processing in the Golgi.[43−45] Interestingly, this difference in processing is not only limited to mammalian core α1,6-fucosyltransferase but also found in plants that modify complex N-glycans with core α1,3-fucose. The absence of plant-specific fucosylation has been observed on the CH2 N-glycan of IgAs expressed in wild-type *N. benthamiana* plants[18,31] and was also found in the present study on recombinant anti-HER2 IgAs when expressed in wild-type plants (data not shown). The local interaction of the complex N-glycan with amino acids from the CH2 domain likely prevents the modification with α1,6- or α1,3-linked fucose. Site-specific N-glycan processing has been observed for several glycoproteins, but the structural polypeptide features that affect these modifications are currently not understood. In this respect, it will be of great interest to perform mutational analysis of the local amino acid environment surrounding the N-glycosylation site and examine the effect on the N-glycan structures. Combined with molecular -modeling experiments this could help us to better understand glycan-processing reactions.

Moreover, in the light of the dramatic effect of the nonfucosylated IgG1 Fc N-glycan on cytotoxicity, it is tempting to speculate that the absence of core fucose on complex N-glycans at this particular position of IgA1 is biologically relevant. A critical role of core fucose for N-glycan processing of immunoglobulins has been recently shown for cetuximab, which carries an N-glycan in the Fab domain in addition to the one in the CH2 domain.[46] While processing of the oligosaccharide in the Fab domain is unaffected by fucosylation, the presence of core fucose leads to increased levels of sialylated Fc glycans. Notably, there is mounting evidence of the antigen-specific generation of immunoglobulin glycoforms during diseases;[47] for example, increased amounts of afucosylated IgGs have been detected on naturally occurring antivirus antibodies of infected patients.[48,49] In summary, these data suggest that the fucosylation of N-glycans on distinct sites of different immunoglobulins is a key determinant of their immunomodulatory functions. The role of this particular nonfucosylated N-glycan in the IgA CH2 domain needs to be further investigated in the future.

Compared with the role of the Fc glycosylation, the importance of N-glycans for interaction of IgM, IgEs, or IgAs with their cellular receptors is less understood.[47] An oligomannosidic glycan at a particular position of the IgE heavy chain has recently been shown to affect IgE binding to the Fcε receptor.[50] Although the N-glycosylation site of the IgA CH2 domain is close to the Fcα receptor binding site and approaches the receptor, there is no contact.[14,44,51] Consequently, it has been proposed that the IgA N-glycans do not contribute to immune effector functions mediated by the Fcα receptor. However, variations in glycosylation may induce subtle conformational changes affecting the overall protein stability or interaction with other receptors, like those involved in protein turnover.[13] Further studies will aim to generate defined IgA glycoforms to unravel the contribution of the glycan composition to protein stability and diverse receptor interactions.

■ ASSOCIATED CONTENT

Supporting Information

The Supporting Information is available free of charge on the ACS Publications website at DOI: 10.1021/acs.jproteome.7b00121.

DOI: 10.1021/acs.jproteome.7b00121
J. Proteome Res. 2017, 16, 2560−2570

Supplementary Figure S1. MS spectra of the tryptic glycopeptides derived from the alpha chain of the purified IgA subtypes. Supplementary Figure S2. MS spectra showing different N-glycan profiles in the two bands derived from the 55 kDa heavy chain. (PDF)

AUTHOR INFORMATION

Corresponding Author

*E-mail: richard.strasser@boku.ac.at. Tel: +43-1-47654-94145.

ORCID

Richard Strasser: 0000-0001-8764-6530

Notes

The authors declare no competing financial interest.

ACKNOWLEDGMENTS

We thank Professor George Lomonosoff (John Innes Centre, Norwich, U.K.) and Plant Bioscience Limited (PBL) (Norwich, U.K.) for supplying the pEAQ-HT expression vector. This work was performed with support of the PhD program BioToP-Biomolecular Technology of Proteins funded by the Austrian Science Fund (FWF Project W1224) and by a grant from the Austrian Federal Ministry of Transport, Innovation and Technology (bmvit) and Austrian Science Fund (FWF): TRP 242-B20.

ABBREVIATIONS

DSC, differential scanning calorimetry; α-HC, alpha heavy chain; HEK, human embryonic kidney; HER2, human epidermal growth factor receptor 2; Ig, immunoglobulin; κ-LC, kappa light chain; LC−ESI−MS, liquid chromatography electrospray ionization mass spectrometry; MALS, multiangle light scattering; MWCO, molecular weight cutoff; SEC, size exclusion chromatography

REFERENCES

(1) Dechant, M.; Beyer, T.; Schneider-Merck, T.; Weisner, W.; Peipp, M.; van de Winkel, J. G.; Valerius, T. Effector mechanisms of recombinant IgA antibodies against epidermal growth factor receptor. *J. Immunol.* **2007**, *179* (5), 2936−43.

(2) Pascal, V.; Laffleur, B.; Debin, A.; Cuvillier, A.; van Egmond, M.; Drocourt, D.; Imbertie, L.; Pangault, C.; Tarte, K.; Tiraby, G.; Cogne, M. Anti-CD20 IgA can protect mice against lymphoma development: evaluation of the direct impact of IgA and cytotoxic effector recruitment on CD20 target cells. *Haematologica* **2012**, *97* (11), 1686−94.

(3) Boross, P.; Lohse, S.; Nederend, M.; Jansen, J. H.; van Tetering, G.; Dechant, M.; Peipp, M.; Royle, L.; Liew, L. P.; Boon, L.; van Rooijen, N.; Bleeker, W. K.; Parren, P. W.; van de Winkel, J. G.; Valerius, T.; Leusen, J. H. IgA EGFR antibodies mediate tumour killing in vivo. *EMBO Mol. Med.* **2013**, *5* (8), 1213−26.

(4) Shields, R. L.; Lai, J.; Keck, R.; O'Connell, L. Y.; Hong, K.; Meng, Y. G.; Weikert, S. H.; Presta, L. G. Lack of fucose on human IgG1 N-linked oligosaccharide improves binding to human Fcgamma RIII and antibody-dependent cellular toxicity. *J. Biol. Chem.* **2002**, *277* (30), 26733−40.

(5) Shinkawa, T.; Nakamura, K.; Yamane, N.; Shoji-Hosaka, E.; Kanda, Y.; Sakurada, M.; Uchida, K.; Anazawa, H.; Satoh, M.; Yamasaki, M.; Hanai, N.; Shitara, K. The absence of fucose but not the presence of galactose or bisecting N-acetylglucosamine of human IgG1 complex-type oligosaccharides shows the critical role of enhancing antibody-dependent cellular cytotoxicity. *J. Biol. Chem.* **2003**, *278* (5), 3466−73.

(6) Nimmerjahn, F.; Ravetch, J. V. Translating basic mechanisms of IgG effector activity into next generation cancer therapies. *Cancer Immun.* **2012**, *12*, 13.

(7) Reusch, D.; Tejada, M. L. Fc glycans of therapeutic antibodies as critical quality attributes. *Glycobiology* **2015**, *25* (12), 1325−34.

(8) Subedi, G. P.; Hanson, Q. M.; Barb, A. W. Restricted motion of the conserved immunoglobulin G1 N-glycan is essential for efficient FcgammaRIIIa binding. *Structure* **2014**, *22* (10), 1478−88.

(9) Rifai, A.; Fadden, K.; Morrison, S. L.; Chintalacharuvu, K. R. The N-glycans determine the differential blood clearance and hepatic uptake of human immunoglobulin (Ig)A1 and IgA2 isotypes. *J. Exp. Med.* **2000**, *191* (12), 2171−82.

(10) Stockert, R. J.; Kressner, M. S.; Collins, J. C.; Sternlieb, I.; Morell, A. G. IgA interaction with the asialoglycoprotein receptor. *Proc. Natl. Acad. Sci. U. S. A.* **1982**, *79* (20), 6229−31.

(11) Yang, W. H.; Aziz, P. V.; Heithoff, D. M.; Mahan, M. J.; Smith, J. W.; Marth, J. D. An intrinsic mechanism of secreted protein aging and turnover. *Proc. Natl. Acad. Sci. U. S. A.* **2015**, *112* (44), 13657−62.

(12) Basset, C.; Devauchelle, V.; Durand, V.; Jamin, C.; Pennec, Y. L.; Youinou, P.; Dueymes, M. Glycosylation of immunoglobulin A influences its receptor binding. *Scand. J. Immunol.* **1999**, *50* (6), 572−9.

(13) Rouwendal, G. J.; van der Lee, M. M.; Meyer, S.; Reiding, K. R.; Schouten, J.; de Roo, G.; Egging, D. F.; Leusen, J. H.; Boross, P.; Wuhrer, M.; Verheijden, G. F.; Dokter, W. H.; Timmers, M.; Ubink, R. A comparison of anti-HER2 IgA and IgG1 in vivo efficacy is facilitated by high N-glycan sialylation of the IgA. *MAbs* **2016**, *8* (1), 74−86.

(14) Herr, A. B.; Ballister, E. R.; Bjorkman, P. J. Insights into IgA-mediated immune responses from the crystal structures of human FcalphaRI and its complex with IgA1-Fc. *Nature* **2003**, *423* (6940), 614−20.

(15) Narimatsu, Y.; Kubota, T.; Furukawa, S.; Morii, H.; Narimatsu, H.; Yamasaki, K. Effect of glycosylation on cis/trans isomerization of prolines in IgA1-hinge peptide. *J. Am. Chem. Soc.* **2010**, *132* (16), 5548−9.

(16) Royle, L.; Roos, A.; Harvey, D. J.; Wormald, M. R.; van Gijlswijk-Janssen, D.; Redwan, E.-R. M.; Wilson, I. A.; Daha, M. R.; Dwek, R. A.; Rudd, P. M. Secretory IgA N- and O-glycans provide a link between the innate and adaptive immune systems. *J. Biol. Chem.* **2003**, *278* (22), 20140−53.

(17) Woof, J. M.; Russell, M. W. Structure and function relationships in IgA. *Mucosal Immunol.* **2011**, *4* (6), 590−597.

(18) Westerhof, L. B.; Wilbers, R. H.; van Raaij, D. R.; Nguyen, D. L.; Goverse, A.; Henquet, M. G.; Hokke, C. H.; Bosch, D.; Bakker, J.; Schots, A. Monomeric IgA can be produced in planta as efficient as IgG, yet receives different N-glycans. *Plant Biotechnol J.* **2014**, *12* (9), 1333−42.

(19) Meyer, S.; Nederend, M.; Jansen, J. H.; Reiding, K. R.; Jacobino, S. R.; Meeldijk, J.; Bovenschen, N.; Wuhrer, M.; Valerius, T.; Ubink, R.; Boross, P.; Rouwendal, G.; Leusen, J. H. Improved in vivo anti-tumor effects of IgA-Her2 antibodies through half-life extension and serum exposure enhancement by FcRn targeting. *MAbs* **2016**, *8* (1), 87−98.

(20) Lohse, S.; Meyer, S.; Meulenbroek, L. A.; Jansen, J. H.; Nederend, M.; Kretschmer, A.; Klausz, K.; Moginger, U.; Derer, S.; Rosner, T.; Kellner, C.; Schewe, D.; Sondermann, P.; Tiwari, S.; Kolarich, D.; Peipp, M.; Leusen, J. H.; Valerius, T. An Anti-EGFR IgA That Displays Improved Pharmacokinetics and Myeloid Effector Cell Engagement In Vivo. *Cancer Res.* **2016**, *76* (2), 403−17.

(21) Plomp, R.; Hensbergen, P. J.; Rombouts, Y.; Zauner, G.; Dragan, I.; Koeleman, C. A.; Deelder, A. M.; Wuhrer, M. Site-specific N-glycosylation analysis of human immunoglobulin e. *J. Proteome Res.* **2014**, *13* (2), 536−46.

(22) Loos, A.; Gruber, C.; Altmann, F.; Mehofer, U.; Hensel, F.; Grandits, M.; Oostenbrink, C.; Stadlmayr, G.; Furtmuller, P. G.; Steinkellner, H. Expression and glycoengineering of functionally active heteromultimeric IgM in plants. *Proc. Natl. Acad. Sci. U. S. A.* **2014**, *111* (17), 6263−8.

DOI: 10.1021/acs.jproteome.7b00121
J. Proteome Res. 2017, 16, 2560−2570

(23) Deshpande, N.; Jensen, P. H.; Packer, N. H.; Kolarich, D. GlycoSpectrumScan: fishing glycopeptides from MS spectra of protease digests of human colostrum sIgA. *J. Proteome Res.* **2010**, *9* (2), 1063−75.
(24) Huang, J.; Guerrero, A.; Parker, E.; Strum, J. S.; Smilowitz, J. T.; German, J. B.; Lebrilla, C. B. Site-specific glycosylation of secretory immunoglobulin A from human colostrum. *J. Proteome Res.* **2015**, *14* (3), 1335−49.
(25) Qiu, X.; Wong, G.; Audet, J.; Bello, A.; Fernando, L.; Alimonti, J. B.; Fausther-Bovendo, H.; Wei, H.; Aviles, J.; Hiatt, E.; Johnson, A.; Morton, J.; Swope, K.; Bohorov, O.; Bohorova, N.; Goodman, C.; Kim, D.; Pauly, M. H.; Velasco, J.; Pettitt, J.; Olinger, G. G.; Whaley, K.; Xu, B.; Strong, J. E.; Zeitlin, L.; Kobinger, G. P. Reversion of advanced Ebola virus disease in nonhuman primates with ZMapp. *Nature* **2014**, *514* (7520), 47−53.
(26) Cho, H.-S.; Mason, K.; Ramyar, K. X.; Stanley, A. M.; Gabelli, S. B.; Denney, D. W.; Leahy, D. J. Structure of the extracellular region of HER2 alone and in complex with the Herceptin Fab. *Nature* **2003**, *421* (6924), 756−760.
(27) Sainsbury, F.; Thuenemann, E. C.; Lomonossoff, G. P. pEAQ: versatile expression vectors for easy and quick transient expression of heterologous proteins in plants. *Plant Biotechnol. J.* **2009**, *7* (7), 682−93.
(28) Durocher, Y.; Perret, S.; Kamen, A. High-level and high-throughput recombinant protein production by transient transfection of suspension-growing human 293-EBNA1 cells. *Nucleic Acids Res.* **2002**, *30* (2), E9.
(29) Strasser, R.; Stadlmann, J.; Schahs, M.; Stiegler, G.; Quendler, H.; Mach, L.; Glossl, J.; Weterings, K.; Pabst, M.; Steinkellner, H. Generation of glyco-engineered Nicotiana benthamiana for the production of monoclonal antibodies with a homogeneous human-like N-glycan structure. *Plant Biotechnol J.* **2008**, *6* (4), 392−402.
(30) Garber, E.; Demarest, S. J. A broad range of Fab stabilities within a host of therapeutic IgGs. *Biochem. Biophys. Res. Commun.* **2007**, *355* (3), 751−7.
(31) Dicker, M.; Tschofen, M.; Maresch, D.; Konig, J.; Juarez, P.; Orzaez, D.; Altmann, F.; Steinkellner, H.; Strasser, R. Transient Glyco-Engineering to Produce Recombinant IgA1 with Defined N- and O-Glycans in Plants. *Front. Plant Sci.* **2016**, *7*, 18.
(32) Paul, M.; Reljic, R.; Klein, K.; Drake, P. M.; van Dolleweerd, C.; Pabst, M.; Windwarder, M.; Arcalis, E.; Stoger, E.; Altmann, F.; Cosgrove, C.; Bartolf, A.; Baden, S.; Ma, J. K. Characterization of a plant-produced recombinant human secretory IgA with broad neutralizing activity against HIV. *MAbs* **2014**, *6* (6), 1585−97.
(33) Strasser, R.; Altmann, F.; Steinkellner, H. Controlled glycosylation of plant-produced recombinant proteins. *Curr. Opin. Biotechnol.* **2014**, *30*, 95−100.
(34) Strasser, R. Plant protein glycosylation. *Glycobiology* **2016**, *26* (9), 926−939.
(35) Shrimal, S.; Trueman, S. F.; Gilmore, R. Extreme C-terminal sites are posttranslocationally glycosylated by the STT3B isoform of the OST. *J. Cell Biol.* **2013**, *201* (1), 81−95.
(36) Zheng, K.; Yarmarkovich, M.; Bantog, C.; Bayer, R.; Patapoff, T. W. Influence of glycosylation pattern on the molecular properties of monoclonal antibodies. *MAbs* **2014**, *6* (3), 649−58.
(37) Yang, Z.; Drew, D. P.; Jorgensen, B.; Mandel, U.; Bach, S. S.; Ulvskov, P.; Levery, S. B.; Bennett, E. P.; Clausen, H.; Petersen, B. L. Engineering mammalian mucin-type O-glycosylation in plants. *J. Biol. Chem.* **2012**, *287* (15), 11911−23.
(38) Castilho, A.; Neumann, L.; Daskalova, S.; Mason, H. S.; Steinkellner, H.; Altmann, F.; Strasser, R. Engineering of sialylated mucin-type O-glycosylation in plants. *J. Biol. Chem.* **2012**, *287* (43), 36518−26.
(39) Karnoup, A. S.; Turkelson, V.; Anderson, W. H. O-linked glycosylation in maize-expressed human IgA1. *Glycobiology* **2005**, *15* (10), 965−81.
(40) Pinkhasov, J.; Alvarez, M. L.; Rigano, M. M.; Piensook, K.; Larios, D.; Pabst, M.; Grass, J.; Mukherjee, P.; Gendler, S. J.; Walmsley, A. M.; Mason, H. S. Recombinant plant-expressed tumour-associated MUC1 peptide is immunogenic and capable of breaking tolerance in MUC1.Tg mice. *Plant Biotechnol J.* **2011**, *9* (9), 991−1001.
(41) Knoppova, B.; Reily, C.; Maillard, N.; Rizk, D. V.; Moldoveanu, Z.; Mestecky, J.; Raska, M.; Renfrow, M. B.; Julian, B. A.; Novak, J. The Origin and Activities of IgA1-Containing Immune Complexes in IgA Nephropathy. *Front. Immunol.* **2016**, *7*, 117.
(42) Parsons, J.; Altmann, F.; Graf, M.; Stadlmann, J.; Reski, R.; Decker, E. L. A gene responsible for prolyl-hydroxylation of moss-produced recombinant human erythropoietin. *Sci. Rep.* **2013**, *3*, 3019.
(43) Tanaka, A.; Iwase, H.; Hiki, Y.; Kokubo, T.; Ishii-Karakasa, I.; Toma, K.; Kobayashi, Y.; Hotta, K. Evidence for a site-specific fucosylation of N-linked oligosaccharide of immunoglobulin A1 from normal human serum. *Glycoconjugate J.* **1998**, *15* (10), 995−1000.
(44) Gomes, M. M.; Wall, S. B.; Takahashi, K.; Novak, J.; Renfrow, M. B.; Herr, A. B. Analysis of IgA1 N-glycosylation and its contribution to FcalphaRI binding. *Biochemistry* **2008**, *47* (43), 11285−99.
(45) Yoo, E. M.; Yu, L. J.; Wims, L. A.; Goldberg, D.; Morrison, S. L. Differences in N-glycan structures found on recombinant IgA1 and IgA2 produced in murine myeloma and CHO cell lines. *MAbs* **2010**, *2* (3), 320−34.
(46) Castilho, A.; Gruber, C.; Thader, A.; Oostenbrink, C.; Pechlaner, M.; Steinkellner, H.; Altmann, F. Processing of complex N-glycans in IgG Fc-region is affected by core fucosylation. *MAbs* **2015**, *7* (5), 863−70.
(47) Plomp, R.; Bondt, A.; de Haan, N.; Rombouts, Y.; Wuhrer, M. Recent Advances in Clinical Glycoproteomics of Immunoglobulins (Igs). *Mol. Cell. Proteomics* **2016**, *15* (7), 2217−28.
(48) Ackerman, M. E.; Crispin, M.; Yu, X.; Baruah, K.; Boesch, A. W.; Harvey, D. J.; Dugast, A. S.; Heizen, E. L.; Ercan, A.; Choi, I.; Streeck, H.; Nigrovic, P. A.; Bailey-Kellogg, C.; Scanlan, C.; Alter, G. Natural variation in Fc glycosylation of HIV-specific antibodies impacts antiviral activity. *J. Clin. Invest.* **2013**, *123* (5), 2183−92.
(49) Wang, T. T.; Sewatanon, J.; Memoli, M. J.; Wrammert, J.; Bournazos, S.; Bhaumik, S. K.; Pinsky, B. A.; Chokephaibulkit, K.; Onlamoon, N.; Pattanapanyasat, K.; Taubenberger, J. K.; Ahmed, R.; Ravetch, J. V. IgG antibodies to dengue enhanced for FcgammaRIIIA binding determine disease severity. *Science* **2017**, *355* (6323), 395−398.
(50) Shade, K. T.; Platzer, B.; Washburn, N.; Mani, V.; Bartsch, Y. C.; Conroy, M.; Pagan, J. D.; Bosques, C.; Mempel, T. R.; Fiebiger, E.; Anthony, R. M. A single glycan on IgE is indispensable for initiation of anaphylaxis. *J. Exp. Med.* **2015**, *212* (4), 457−67.
(51) Mattu, T. S.; Pleass, R. J.; Willis, A. C.; Kilian, M.; Wormald, M. R.; Lellouch, A. C.; Rudd, P. M.; Woof, J. M.; Dwek, R. A. The glycosylation and structure of human serum IgA1, Fab, and Fc regions and the role of N-glycosylation on Fcalpha receptor interactions. *J. Biol. Chem.* **1998**, *273* (4), 2260−72.

DOI: 10.1021/acs.jproteome.7b00121
J. Proteome Res. 2017, 16, 2560−2570